Experimental Modelling of the Caprock/Cement Interface Behaviour under CO2 Storage Conditions: Effect of Water and Supercritical CO2 from a Cathodoluminescence Study

Emmanuel Jobard, Jérôme Sterpenich, Jacques Pironon, Jérôme Corvisier, Aurélien Randi

geosciences

MDPI

Article

Experimental Modelling of the Caprock/Cement Interface Behaviour under CO_2 Storage Conditions: Effect of Water and Supercritical CO_2 from a Cathodoluminescence Study

Emmanuel Jobard [1], Jérôme Sterpenich [1,*], Jacques Pironon [1], Jérôme Corvisier [1,2] and Aurélien Randi [1]

[1] Laboratoire GeoRessources, Université de Lorraine, UMR 7359, BP 70239, 54506 Vandoeuvre lès Nancy, France; emmanuel.jobard@gmail.com (E.J.); jacques.pironon@univ-lorraine.fr (J.P.); jerome.corvisier@mines-paristech.fr (J.C.); aurelien.randi@univ-lorraine.fr (A.R.)

[2] Mines Paristech, 35 rue Saint Honoré, 77305 Fontainebleau CEDEX, France

* Correspondence: jerome.sterpenich@univ-lorraine.fr; Tel.: +33-3-7274-5659

Received: 11 April 2018; Accepted: 15 May 2018; Published: 18 May 2018

Abstract: In the framework of CO_2 geological storage, one of the critical points leading to possible important CO_2 leakage is the behaviour of the different interfaces between the rocks and the injection wells. This paper discussed the results from an experimental modelling of the evolution of a caprock/cement interface under high pressure and temperature conditions. Batch experiments were performed with a caprock (Callovo-Oxfordian claystone of the Paris Basin) in contact with a cement (Portland class G) in the presence of supercritical CO_2 under dry or wet conditions. The mineralogical and mechanical evolution of the caprock, the Portland cement, and their interface submitted to the attack of carbonic acid either supercritical or dissolved in a saline water under geological conditions of pressure and temperature. This model should help to better understand the behaviour of interfaces in the proximal zone at the injection site and to prevent risks of leakage from this critical part of injection wells. After one month of ageing at 80 °C under 100 bar of CO_2 pressure, the caprock, the cement, and the interface between the caprock and cement are investigated with Scanning Electron Microscopy (SEM) and cathodoluminescence (CL). The main results reveal (i) the influence of the alteration conditions: with dry CO_2, the carbonation of the cement is more extended than under wet conditions; (ii) successive phases of carbonate precipitation (calcite and aragonite) responsible for the loss of mechanical cohesion of the interfaces; (iii) the mineralogical and chemical evolution of the cement which undergoes successive phases of carbonation and leaching; (iv) the limited reactivity of the clayey caprock despite the acidic attack of CO_2; and (v) the influence of water on the transport mechanisms of dissolved species and thus on the location of mineral precipitations.

Keywords: CO_2 storage; Portland cement; clays; caprock; interface; well integrity; high-pressure experiment

1. Introduction

Under CO_2 storage conditions at temperatures from around 25 to 150 °C and pressures from around 80 to 400 bar, the behaviour of the different materials used in a CO_2 geological storage site is a key factor to consider for safe sequestration. Risks of leakage are considered to be more likely located at the interface between well materials and rocks, of both reservoirs and caprocks [1]. Cement used adjacent to the casing of injection wells is known as a critical material because of its chemical reactivity, especially with CO_2, leading to its carbonation. Many studies focused on well cement

reactivity are available in the literature. Some of them describe samples collected from real CO_2 storage sites (e.g., [2–4]). These studies show that despite the strong reactivity of the cement phase, its integrity is preserved and prevents the CO_2 from migrating through the casing up to the atmosphere. A second type of studies is devoted to experimental simulations (e.g., [5–8]). Samples of cement are aged under high CO_2 pressure and at different temperatures. Some studies focus on cement/rock interfaces, with the rock being sandstones (e.g., [9–11] Cao, Walsh, Mito), basalts (e.g., [12] Jung), shales (e.g., [4,13]), siltstones (e.g., [14] Newell), or claystones (e.g., [15] Manceau).

As observed in physical case studies, experimental modelling with cement samples shows the same phenomenon of calcium-silicate-hydrate (C-S-H) dissolution/carbonation involving the formation of moving reactive fronts (e.g., [16,17]) and carbonation. Despite the introduction of CO_2 resistant cement [18], which results in the disappearance of an alteration front that may impair its mechanical integrity, the cement carbonation still remains the main concern of the scientific community. One possibility is the cement mainly fracturing at the interface with well materials or rocks (caprock and reservoir rock), which could allow a migration of the CO_2 toward the atmosphere. Angeli et al. [19] experimentally reproduced CO_2 flow through the Draupne Formation (Upper Jurassic of the Northern North Sea) and highlighted the re-opening of microfractures, allowing the CO_2 migration along high-permeability pathways. Similar results were obtained from the numerical study by Rutqvist and Tsang [20]. Moreover, in order to predict the evolution of storage sites over extended scales of time and space, these experimental simulations are essential to provide data for the validation of numerical simulations (e.g., [21,22]). Unfortunately, most of the existing papers are focused on the integrity of one material only, cement or rock, or do not consider the mechanical effects of cement transformation. However, the interfaces between the different materials which comprise a CO_2 storage system represent a physico-chemical area of weakness. Wigand et al. [23] studied the assemblage of fractured cement and powdered shale in the presence of supercritical CO_2 (54 °C and 199 bar) and then highlighted the absence of significant reactions at the cement/caprock interface. Duguid [24] showed the strong chemical reactivity of the cement/sandstone interface, but in this experiment, no fracturing or any other physical impairment was observed. The lack of studies concerning the behaviour of interfaces in CO_2 storage site conditions led us to develop an original designed batch experiment at the GeoRessources laboratory (Université de Lorraine, France). In this study, the reactivity between the caprock and cement was carried out under dry conditions or with an aqueous solution. A petrographic study of rock, cement, and their interfaces using cathodoluminsecence and Scanning Electron Microscopy observations was carried out to follow the mechanical and mineralogical evolution of the interface due to mineral transformations. In particular, different phases of carbonation were highlighted and a chronology of the cement impairment was established.

2. Materials and Methods

In order to study the behaviour of the cement/caprock interface, original batch experiments were designed. The clayey rock of a Callovo-Oxfordian age (COX) was selected to represent the caprock in this experiment. This geological stratum is intensively studied within the framework of the geological storage of nuclear waste in France (ANDRA; e.g., [25–27]). XRD analyses of the Callovo–Oxfordian clay rock reveal a dominant argillaceous phase (45% illite and interstratified illite/smectite), a calcium carbonate phase, mainly calcite (25%), and a siliciclastic phase, mostly quartz (25%). Other phases (feldspar, pyrite) and organic matter have been observed, but in mass quantities of less than a few percent [28]. The cement studied is class G Portland cement and was prepared according to the API-ISO 10426A norm (349 $\pm$ 0.5 g of water mixed with 792 $\pm$ 0.5 g of cement). This cement is classically used in the petroleum industry and is also the subject of several works on the geological storage of CO_2 (see for example [29]). The hydrated cement is mainly composed of residual bi/tri calcic silicate (C2S, C3S), portlandite ($Ca(OH)_2$), and a fibrous matrix of calcium silicate hydrated (CSH), which confers its mechanical properties. The samples were prepared according to the following protocol. Firstly, a piece of caprock (25 $\times$ 17 $\times$ 10 mm) was placed in the middle of a silicone mold (35 $\times$ 30 $\times$ 20, Figure 1).

The caprock was previously hydrated for one hour with deionized water in order to prevent cement fracturing during the drying phase. Then, the cement paste was added to fill the mold. The samples were set for 24 h at ambient temperature and finally were removed from the mold.

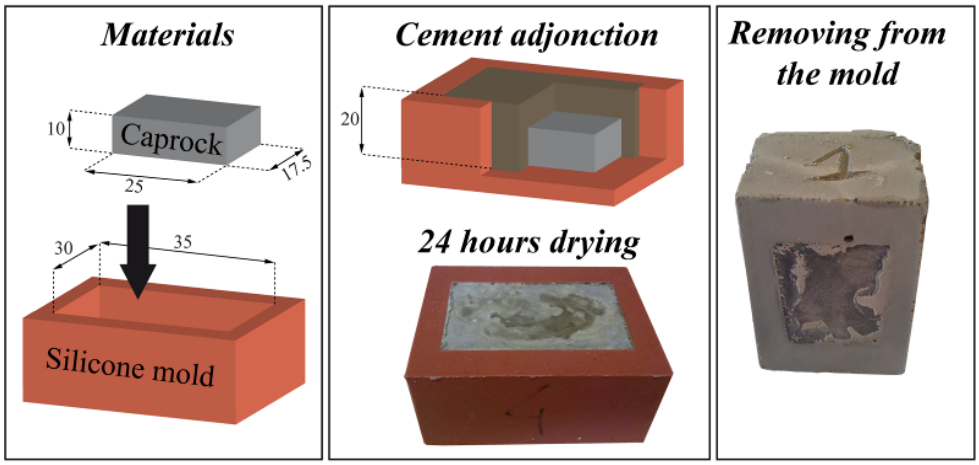

Figure 1. Schematic describing the different steps for the sample preparation (measures are in mm).

The samples were then placed vertically into a 250 mL reactor (Figure 2). The first step of the experiment was curing the samples for seven days in an aqueous solution composed of deionized water with 30 $g \cdot L^{-1}$ of NaCl. The cure consists of the hydration of the samples in the ageing conditions of pressure and temperature (100 bar and 80 °C). At the end of the cure, the reactor was depressurized and one sample was removed (as a blank sample). The reactor was re-pressurized at 100 bar and re-heated at 80 °C, and the ageing lasted for 30 days. During the cure and ageing processes, temperature was regulated but pressure was only monitored. The experiments were carried out with and without the aqueous solution (Figure 3), and with CO_2 or N_2 (selected as an inert gas). Samples aged with N_2 were compared to samples aged in the presence of CO_2. In total, eight samples were tested and analyzed. During the cure, the W/R ratio (ratio between the mass of water and the total mass of solid: cement paste + caprock) ranged from 1.66 to 1.95 and varied between 1.88 and 2.34 during the ageing.

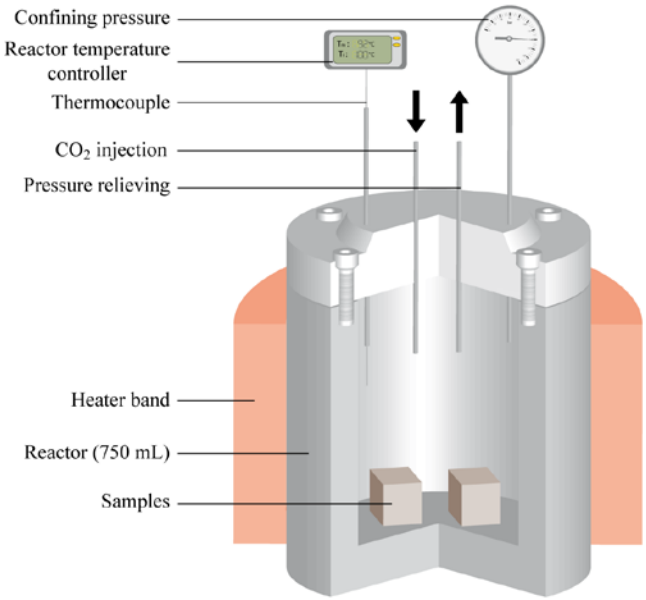

Figure 2. Batch autoclave used for experiments.

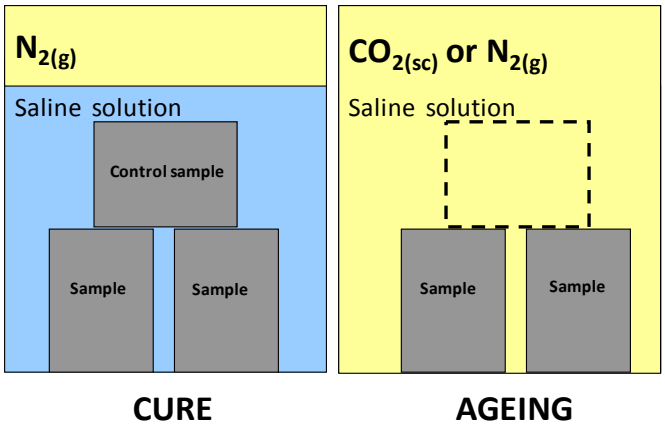

Figure 3. Experimental protocol. On the left side, cure conditions: the samples are completely immersed in the saline solution with an N_2 gas cap. On the right side, after the cure, one sample is removed from the reactor for the initial state study and the remaining samples are aged either under dry conditions or with a saline solution. The gases are N_2 (blank experiment) and CO_2.

3. Analytical Protocol

3.1. Pressure and Temperature Monitoring

In a closed reactor, temperature and pressure are strongly linked, and their variations often indicate that a chemical reaction is occurring. The main reactions which could occur in the reactor and that could influence the total pressure of the system are CO_2 solubilisation (Equation (1)), and, as a function of pH conditions, its dissociation in carbonic acid and bicarbonate ions (Equations (2) and (3) respectively), the dissociation of bicarbonate ions in carbonate ions (Equation (4)), and carbonate precipitation (Equations (5) and (6)). In order to follow these reactions and the potential mineralogical changes, the pressure and the temperature in the reactor were recorded continuously for the entire duration of the experiments, with a step of 3 min. The temperature was also regulated over the entire course of the experiment.

$$CO_{2(g)} = CO_{2(aq)} \quad (1)$$

$$CO_{2(aq)} + H_2O_{(aq)} = H_2CO_{3(aq)} \quad (2)$$

$$H_2CO_{3(aq)} = H^+ + HCO_3^- \quad (3)$$

$$HCO_3^- = H^+ + CO_3^{2-} \quad (4)$$

$$CaCO_{3(s)} + H^+ = Ca^{2+} + HCO_3^- \quad (5)$$

$$CaCO_{3(s)} = CO_3^{2-} + Ca^{2+} \quad (6)$$

3.2. Mass Balance

A mass balance was calculated for each sample before and after ageing in order to estimate the influence of the mineralogical transformation of the system. The mass of the samples aged in the presence of N_2 was measured and compared with the mass of the samples aged in the presence of CO_2. Two weighing procedures were carried out: the first 24 h after the sample was prepared and set at room temperature, and the second at the end of the experiment and after drying at ambient temperature for 24 h. Weighing was performed on a weigh scale with an error of 0.01 g.

3.3. Petrography

A petrographic study was carried out on the samples to highlight mineralogical and morphological transformations. A Scanning Electron Microscopy (SEM) study was carried out on

fresh samples and on polished surfaces (after epoxy resin impregnation). The back scattered electron (BSE) mode was used to study the polished surface of samples. The equipment used was a HITACHI S-4800 SEM with a field effect (SCMEM GeoRessources Laboratory, Université de Lorraine, France). Images were acquired with a voltage of 10 to 15 kV.

A cathodoluminescence microscopy study of samples aged with CO_2 allows monitoring of the crystallisation phases of carbonates. The microscope used was an Olympus BX50 with a Zeiss® Axio CAM MRC image acquisition system. Images were acquired with a 500 µA gun current and a 15 kV voltage.

4. Results

4.1. Pressure and Temperature Monitoring

The pressure and temperature monitored during the entire duration of the experiment are the first available data (Figure 4). These two parameters allow, in the batch experiment, to visualize any significant chemical change in the reactor. For each experiment (N_2 with and without solution, CO_2 with and without solution), the temperatures are constant at 80 °C. Concerning the N_2 experiments, after a rapid pressure decrease, the system reaches an equilibrium state. The decrease of the initial pressure is 3 bar with aqueous solution, and 1 bar without solution. Concerning the ageing with CO_2 with and without aqueous solution, the decrease of the pressure is more important. It is 9 bar with solution and 6 bar without solution. The pressure decrease is faster during the first hours of the experiment, and then it slows down. The decrease is continuous for the experiment with solution but the pressure reaches a sill after 200 h for the experiment with dry CO_2.

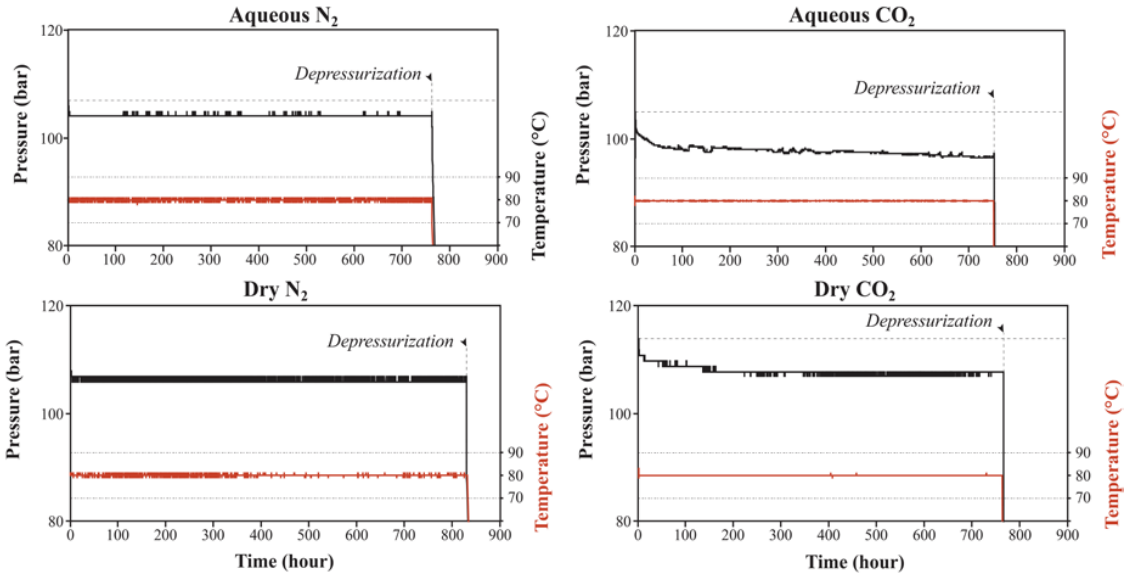

Figure 4. Pressure (**black line**) and temperature (**red line**) monitoring. (**Left**): N_2 experiments. (**Right**): CO_2 experiments.

4.2. Petrography

4.2.1. Observations at the Macroscopic Scale

Observations at the macroscopic scale (Figure 5) reveal the strong fracturing of the samples aged with CO_2, whereas the samples aged with N_2 seem to be preserved. The fracturing should not be due to decompression due to degassing since samples aged with N_2 are intact. For experiments with N_2, the aspect of samples after aging is comparable with or without aqueous solution. Small white crystals have grown on the cement surface. A weak fracturing is also visible on the corner of the cement sheath.

Concerning the samples aged with CO_2, observations show that the cement has turned to an orange to brown colour. The sample aged in the aqueous solution is strongly fractured and the cracking affects both rock and cement. This fracturing leads to the fragmentation of the sample. In the presence of dry CO_2(sc), the sample is also strongly fractured but it essentially affects the cement part.

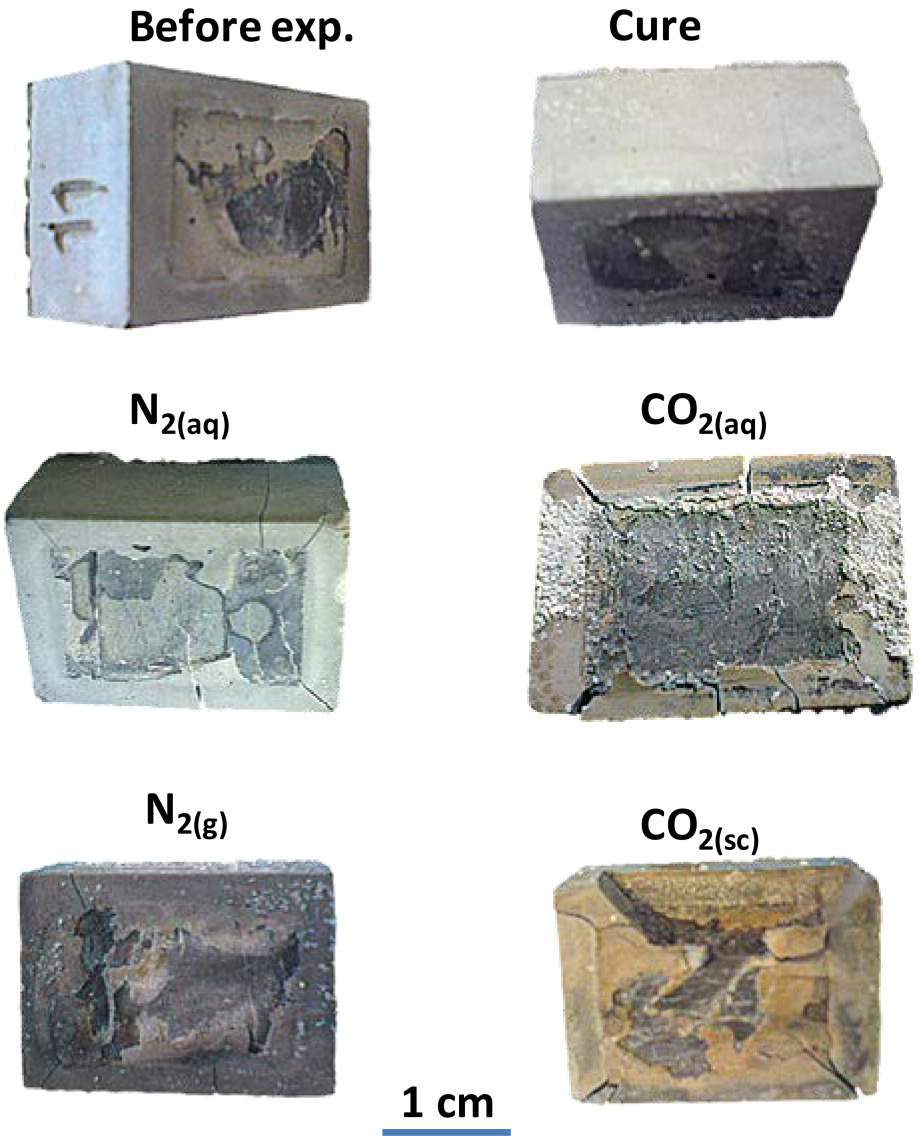

Figure 5. Macroscopic view of the samples after the experiment. Before the experiment, after the cure, with only dry gases (g and sc) and with the presence of aqueous solution (aq).

4.2.2. Observations at the Microscopic Scale

Polished cross-sections were prepared to observe the internal part of the samples, especially the interface between the caprock (COX) and cement. Samples aged with N_2 were observed with SEM, while samples aged with CO_2 were observed with both SEM and cathodoluminescence (CL) devices. Observations of the interface between COX and cement reveal a good mechanical cohesion of the interface for N_2 experiments (Figure 6). For CO_2 experiments, the interface is open and crystallization is observed for experiments with and without aqueous solution.

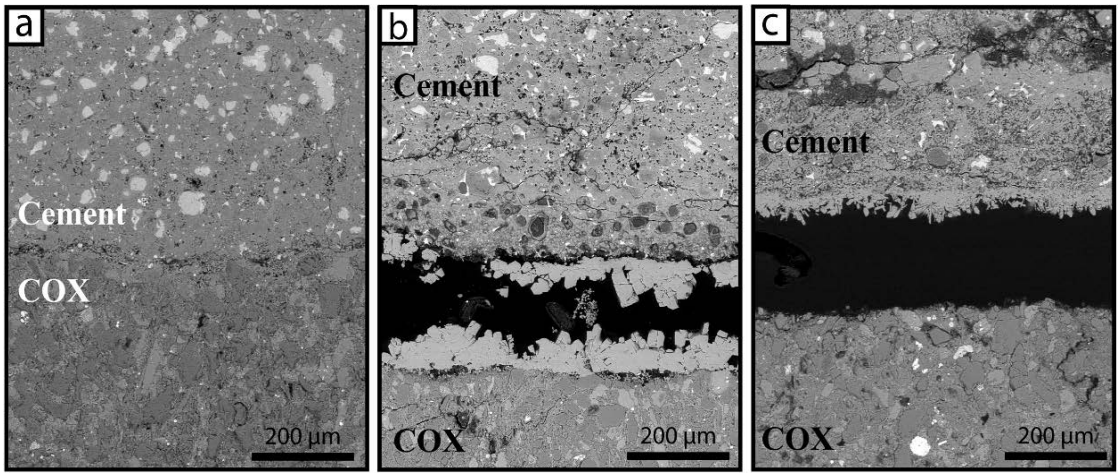

Figure 6. SEM observations of the cement/caprock (COX) interface (back-scattered electrons). (**a**) N_2 + solution experiment; (**b**) CO_2 + solution experiment; (**c**) dry $CO_{2(sc)}$ experiment.

For the experiment with CO_2 and solution (Figure 6b), carbonate crystals precipitated in the fracture at the interface. It is important to notice that these crystals grow on both cement and COX sides. The size of carbonate crystals ranges from 10 to 100 µm. In the cement, a front of carbonation of 100–200 µm thick is also characterized by the presence of dark grey phases, which are most likely leached C2S or C3S grains. Calcium carbonate also precipitated at the rock/cement interface in the dry CO_2(sc) experiment (Figure 6c). With a size of about 10 µm, these crystals are smaller than those observed during the experiment with water. But in this configuration, the carbonation of the interface occurs only on the cement side. A more precise study of carbonation was made with the help of CL microscopy (Figure 7). Three areas of interest were investigated: (1) the rock/cement interface; (2) the cracks in the cement; and (3) the external border of the cement which is assumed to be in contact with CO_2 throughout the experiment.

Concerning the cement/caprock interface, for the CO_2 + solution experiment, (Figure 7a,b) SEM and CL studies highlight (i) the cracks occurring at the interface as well as in the cement sheath; (ii) the carbonation of the cement/caprock interface (orange-red phases on the bottom-left part of the picture) in the clays and filling micro-cracks in the cement); (iii) the carbonation of the cement phase (dark part of the cement in CL, around 100–200 µm thick) where leached C2S and C3S give patches of silica. This zone is complex with different fronts of different densities and chemical composition; (iv) the precipitation of calcium carbonate crystals on both sides of the crack in the cement (edging with green luminescence).

For the experiment with dry CO_2(sc), the carbonation at the interface caprock/cement (Figure 7c,d) is comparable to that with solution. The same altered cement front (carbonation + dissolution) is visible with both SEM and CL but to a larger extent (thickness of 280 µm). The other difference is that the carbonation only occurs at the cement side of the interface.

In order to better constrain the chronology of the complex evolution of the samples, the observation was focused on cracks in the cement sheath. Observed carbonation profiles are similar to those observed on the caprock/cement interface. With the aqueous solution (Figure 7e,f), the alteration of the cement occurs according to a front (dissolution + carbonation) of about 80 µm thick. The "red" carbonation phase is not present in the fracture. Only the "green" phase develops on both sides of the crack. It is of note that the crack opening is larger close to the caprock/cement interface (left side) than close to the external side of the cement sheath (right side). This can be used to interpret the direction of the crack propagation. With dry CO_2(sc) (Figure 7g,h), the two phases of carbonation are observed in the cement. The alteration front presents a variable thickness and covers

a range from 150 µm (right side) to 500 µm (right side). As with the solution, the crack is larger close to the interface with the caprock.

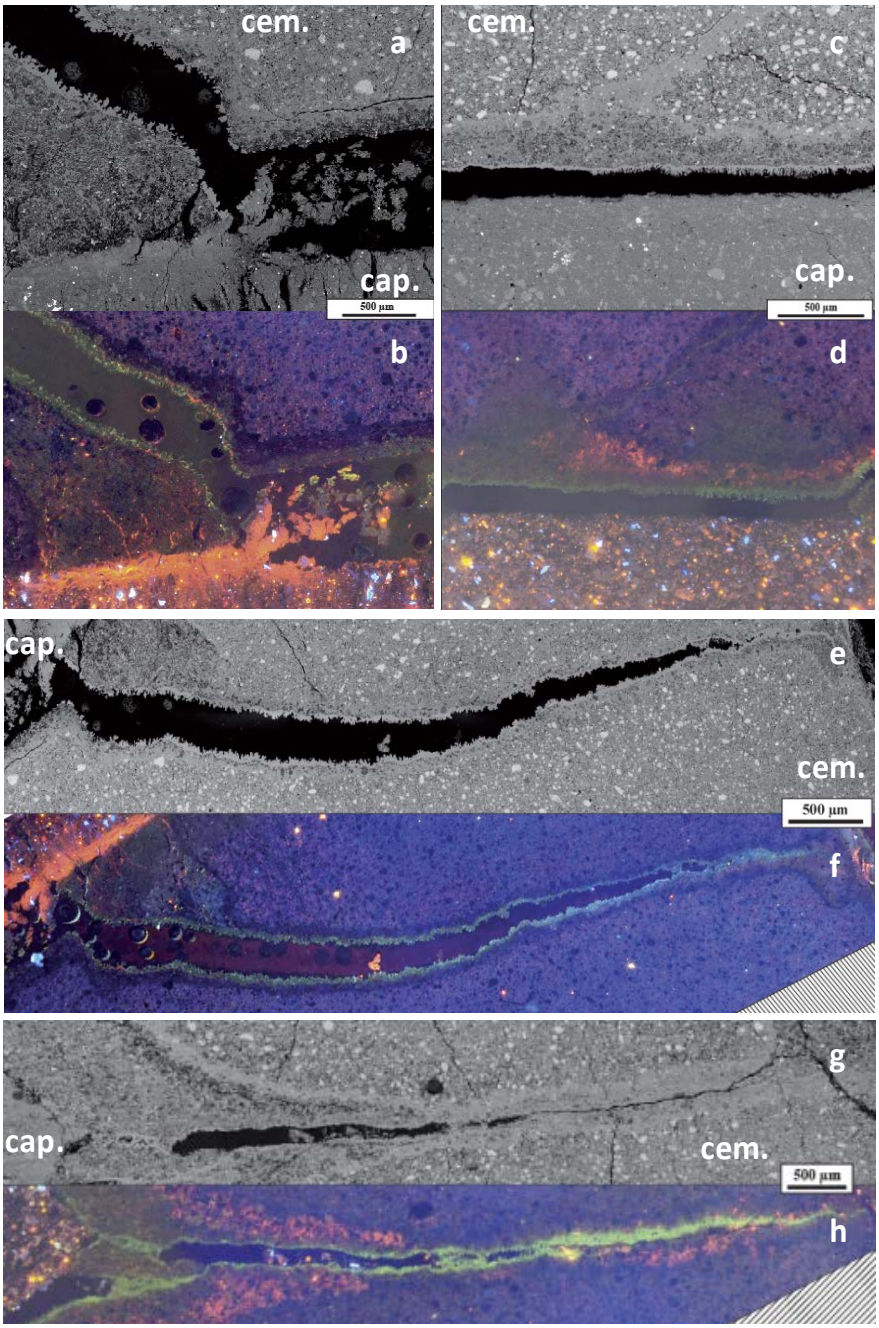

Figure 7. Comparison between SEM (backscattered electrons) and cathodoluminescence (CL) observations. (**a**,**b**) Observations of cracks at the cement (cem.)/caprock (cap.) interface and in the cement after ageing with CO_2 and solution; (**c**,**d**) Observations of the cement/caprock interface after ageing with dry CO_2(sc); (**e**,**f**) Observation of a crack in the cement sheath in a sample aged with CO_2 and solution; (**g**,**h**) Observation of a crack in the cement sheath in a sample aged with dry CO_2(sc).

The observation of the external part of the cement directly in contact with either dry CO_2(sc) or CO_2 + solution gives information on the mechanisms of cement alteration. In particular, measurement of the alteration front provides constraints on the fracture genesis and on the kinetics of the propagation

front. Concerning the experiment with aqueous solution (Figure 8a,b), the carbonation front in the cement is on average 160 µm thick. Notice that no "red" carbonates are present from the CL image observation (Figure 8b). For the experiment with dry CO_2(sc) (Figure 8c,d) the alteration front is thicker: 700 to 1000 µm. Here, the "red" carbonates are characteristic of the altered cement.

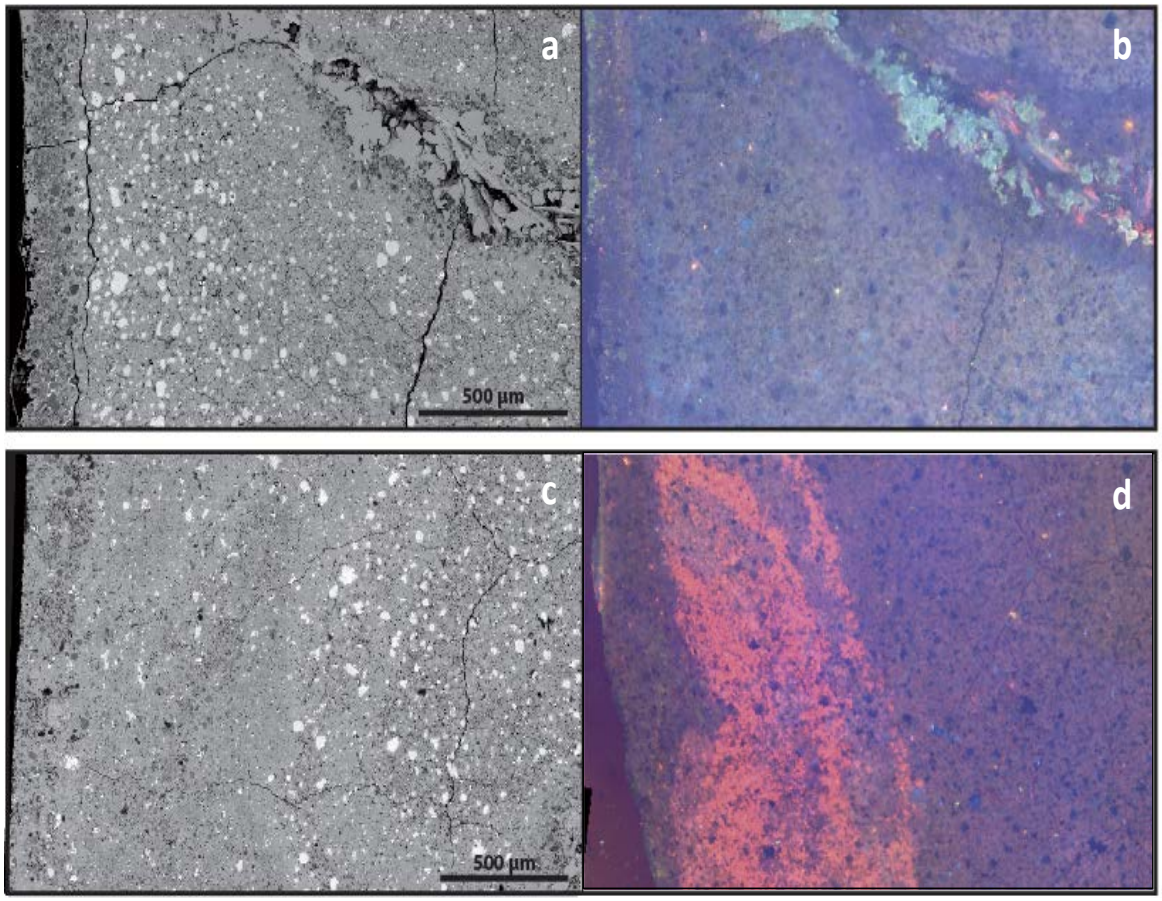

Figure 8. Comparison of observations with SEM (BSE) and CL. External part of the cement sheath in contact with the gas or the aqueous solution. (**a**,**b**) samples aged with CO_2 + solution; (**c**,**d**) samples aged with dry CO_2(sc).

4.3. Mass Balance

The carbonation level of samples can be evaluated by a mass balance performed by weighing the samples before and after the experiment. The initial weight was obtained 24 h after sample preparation and after exposition at ambient temperature. The final mass was measured 24 h after the end of experiment, also after drying at ambient temperature. Notice that the remaining amount of water after drying can vary from one sample to another and has to be considered as the main uncertainty of the mass balance. The results of weighing, as a percentage of the initial mass for the different samples, are given in Figure 9. The mean gain of 1.7% for the samples aged with N_2 + solution is probably due to the hydration of the sample (cement phases mainly) after one month of the experiment. In contrast, the mean loss of 1.8% in mass of the samples aged with dry N_2 can be explained by the dehydration caused by the evaporation of water coming from the porosity of the samples heated at 80°C for one month. Considering that a fluctuation of about ±1.8% can be attributed to hydration/dehydration phenomena, some significant differences still remain if looking at the mass balance of the samples aged with CO_2. A mean gain of 6.7% in mass for the experiment with the solution and of 8.7% for the dry experiment indicates the level of cement carbonation. This mass balance confirms that the

carbonation of the samples aged with CO_2 under dry conditions is more extensive than that with the aqueous solution.

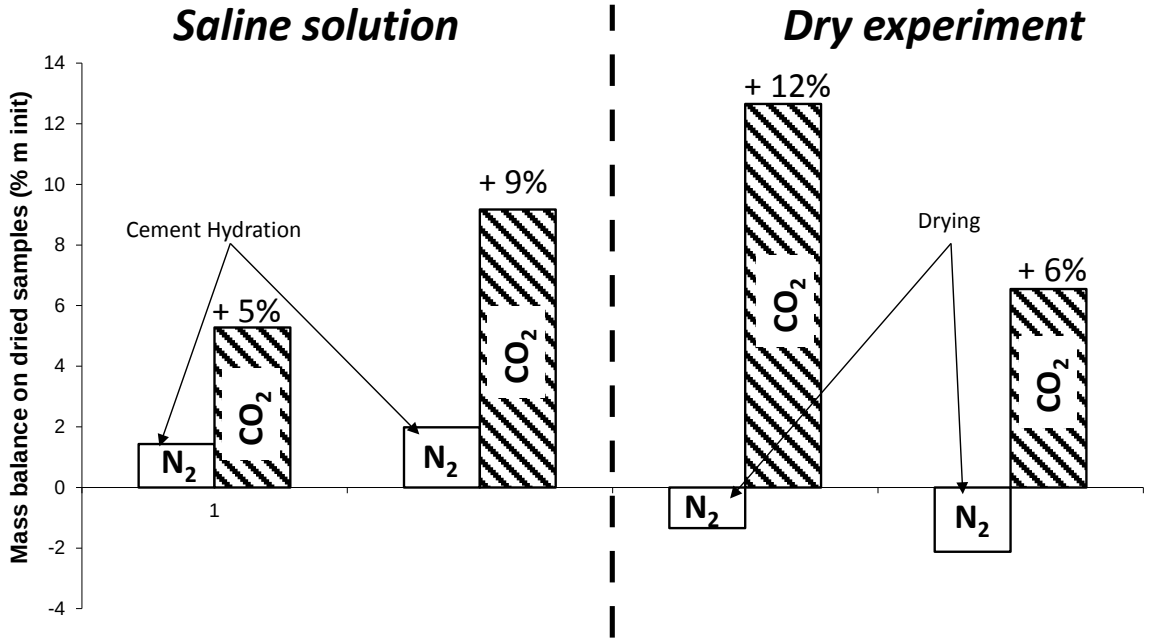

Figure 9. Mass balance of the samples after experiments. Two samples are weighed for each experimental condition.

5. Discussion

The dissolution of CO_2 in the system leads to the formation of carbonic acid (Reaction (2)), which causes the acidification of the environment and its carbonation. The carbonation of the cement is possible thanks to chemical reactions with calcium-bearing phases, portlandite ($Ca(OH)_2$, Reaction (7)), and calcium silicate hydrates (CSH, Reaction (8)).

$$Ca(OH)_2 + H^+ + HCO_3^- = CaCO_3 + 2H_2O \quad (7)$$

$$CSH + H^+ + HCO_3^- = CaCO_3 + SiO_2, nH_2O \quad (8)$$

From the observation of the cement and of the caprock/cement interface, three main steps of carbonation occurred in experiments performed with CO_2. The different zones are illustrated in Figure 10 and are in agreement with the literature (e.g., [9]). The numbering of zones is taken from Sterpenich et al. [7], adapted from Kutchko et al. [16]. The first carbonation phase described is associated with calcium leaching from the cement, which corresponds to zones Z2 and Z3. Z3 is the zone at the interface with the fresh cement; it corresponds to a calcium-depleted zone due to portlandite dissolution and CSH leaching. Z2 is just behind Z3 and is the zone of the first carbonation (dark zone in CL) among the remaining CSH matrix. It is of note that in this same zone, ghosts of C2S or C3S replaced by hydrated silica and which can be considered as a source of calcium for the surrounding carbonates are present. The second phase is represented by the carbonates with a red to orange luminescence (C1) and widely affects the claystone located close to the caprock/cement interface. The third phase is represented by the carbonates with the green luminescence (C2) with an aragonite shape which covers the walls of the cracks. Z1 corresponds to a porous zone and is the result of a partial dissolution of precipitated carbonates and the dominance of hydrated silica. The luminescence colours of C1 and C2, red and green, respectively, indicate that C1 is likely calcite, and C2 aragonite [30,31], which is consistent with other published studies on cement carbonation.

To sum up, the evolution of the sample follows three main steps. In the first step, a front of carbonation develops in the cement sheath (Z2 and Z3). The precipitation of carbonates is due to calcium leaching from CSH and C2S/C3S phases, which combines with aqueous carbonate ions. The changes in volume in the cement paste due to CSH modification (Ca/Si decreases with leaching) and to precipitation of carbonate minerals among the cement paste lead to the cracking of the interface. A second phase of carbonation (C1) grows together with the initial front. The precipitation of carbonate minerals (calcite and aragonite) plays the role of a calcium pump and increases the leaching of CSH, thus leading to changes in volume causing fractures to spread. In a third step, aragonite (C2) covers the two previous fronts of carbonation. The different carbonate generations are directly linked to the evolution of the solution chemistry, and in particular to the increase of the Mg/Ca ratio. De Choudens-Sanchez & Gonzales [32] showed that a strong Mg/Ca ratio could lead to the precipitation of only aragonite crystals. According to these authors, the more the Mg/Ca ratio is high, the more the solution has to be oversaturated to precipitate calcite. The variations of the Mg/Ca ratios during the experiment with the CO_2 + solution are highlighted by Jobard [33]. In his study, he shows that the periphery of carbonate minerals precipitated in the cracks is enriched in Mg in comparison to the core of the crystals. The chemical analysis of the solution in a similar experiment carried out by Jobard [33] also shows that the Mg/Ca increases with time during ageing.

Several fracturing phases were highlighted and occurred at different times. By comparing the thickness of the alteration front measured on the external border of the cement with the rest of the sample, it is possible to determine the fracturing chronology. The external border of the cement was in contact with CO_2 throughout the experiment, whereas it is assumed that the other parts on the cement are preserved from alteration before cracking. For the samples aged with CO_2 + solution, the thickness of the alteration front in the cement is 200 μm at the external border, while it is 160 and 80 μm at the interface with the caprock and in the cement crack, respectively. The mean rate of cement carbonation can be calculated considering an alteration time of 760 h. The mean rate of alteration is 0.26 $\mu m \cdot h^{-1}$, so, considering linear kinetics of alteration, the interface and the cement crack are supposed to be exposed to alteration for around 615 and 308 h, respectively. Thus, the interface cracking should occur after 145 h of alteration, and the cement cracking after 452 h following the CO_2 injection.

The same calculation concerning the samples aged with dry CO_2(sc) gives an alteration rate of 1.2 $\mu m \cdot h^{-1}$ (1000 μm for 835 h of alteration), which is 4.5 times faster than for the experiment with water, producing interface cracking after around 418 h. The cement cracking is more difficult to estimate because the alteration front is not homogeneous and could indicate a slower fracture propagation. An alteration front thickness of around 500 μm presents cement cracking rather contemporary to that of the interface.

A strong difference is visible between the samples with dry CO_2(sc) or with the solution. Under dry conditions, the carbonates only precipitate on the cement side of the interface, showing the importance of the transport mechanisms in mineral precipitation. The penetration of supercritical CO_2 in the cement is more efficient than that of dissolved CO_2 due to the highest CO_2 concentration in the CO_2(sc) experiment, implying a more extended carbonation. In parallel, without aqueous solution, the transport of ions is limited, especially Mg and Ca, leading to local precipitation, whereas with aqueous solution, the ions can be transported in the system and carbonation can occur in the caprock for instance.

The previous calculations support several assumptions, such as the linear kinetics of alteration or the absence of a diffusion barrier linked to carbonate precipitation [34]. However, they give primary information about the fracturing genesis in the samples for the two studied conditions. These results are in agreement with the study of Wigand et al. [23]. The authors suggest a carbonation phase causing the opening of fracture in the cement, which is then sealed by a second phase of calcite precipitation locally leading to a partial fracture closing. But the changes in volume of CSH phases due to Ca leaching also have to be evoked to explain the origin of fracking. The alteration rates reported in the literature cover a broad range which strongly depends on the experimental set up. Duguid,

Andac and Glasser, and Barlet-Gouédard et al. [24,35,36] obtained an alteration rate of 0.125, 0.32, and 0.63 μm·h^{-1}, respectively. Kutchko et al. and Rimmelé et al. [16,37] obtained an alteration rate of about 2 and 30 μm·h^{-1}, respectively. As emphasized by Duguid [24], the alteration rate of the cement in a real case storage is slower than the slowest rate exposed here (e.g., [2]) and strongly depends on the cement quality. They calculate a real degradation rate of 4×10^{-6} to 9×10^{-5} μm·h^{-1}.

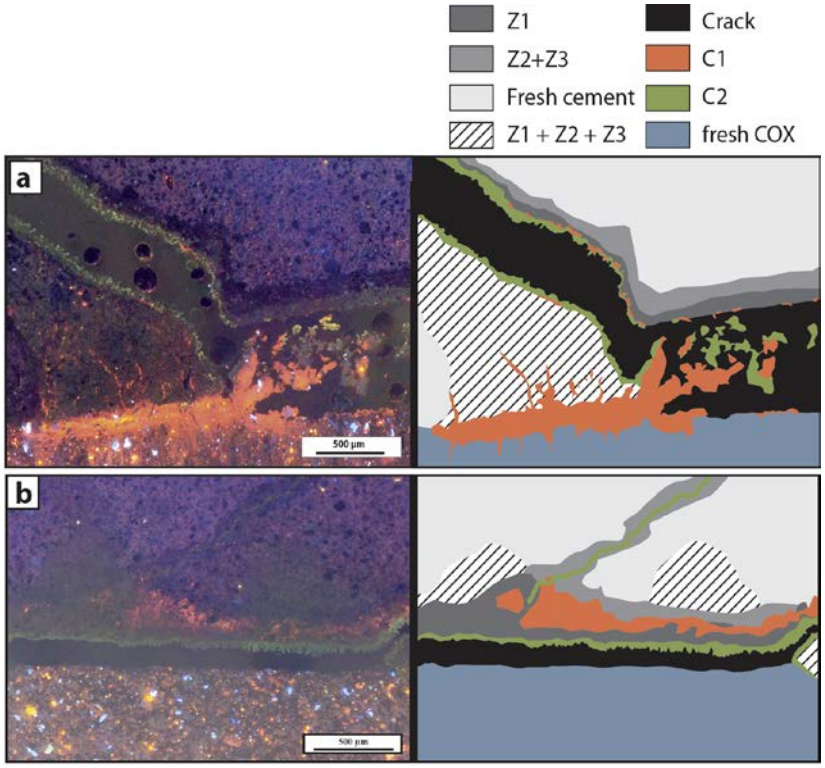

Figure 10. CL image and schematics describing the different phases which affect the caprock/cement interface and the cement after ageing with CO_2. (**a**): experiment CO_2 + solution. (**b**): experiment with dry $CO_{2(sc)}$.

Because samples were weighed before and after the experiment and because the pressure was monitored during experiments, a complete mass balance can be performed. During the two first hours of the experiment with saline solution, the pressure decrease (Figure 2) can be associated with CO_2 dissolution (Reaction (1)). The pressure decrease rate is 0.10 bar·min^{-1}, whereas during the rest of the experiment, it is 1.38×10^{-4} bar·min^{-1}. After CO_2 solubilisation, the fall of pressure is about 2 bar, which corresponds to 2% of the initial pressure. Considering the volume of the samples (30.60 cm^3), the volume of the solution (118 cm^3), and the total volume of the reactor (250 cm^3), it is possible to calculate the volume of the gaseous phase in the system (101.4 cm^3). Assuming that the gas phase is mainly CO_2(sc) with a molar volume of 38.05 cm^3·mol^{-1} (at 80 °C, 100 bar), the entire gas volume corresponds to 2.6 mole of CO_2. A decrease of 2% of the total pressure corresponds to a consumption of 0.052 mol of CO_2. In parallel, the sample weighing gave a mass gain of 4.57 g. The error due to hydration is estimated at +2.1 g from the samples aged in the presence of N_2. The mass gain can be considered to be 2.47 g, corresponding to the precipitation of 0.041 mol of calcite, which is consistent with the value from CO_2 consumption. Concerning the samples aged with dry CO_2(sc), the fall of pressure is assumed to only be associated with CO_2 consumption. The pressure decrease is 3 bar and corresponds to 2.5% of the initial pressure and to a consumption of 0.12 mol of CO_2. The mass balance reveals a gain of 7.37 g, revised according to the weighing of N_2 blank samples.

This corresponds to the precipitation of 0.12 mol of calcite, which is in perfect agreement with the values from CO_2 consumption.

For the same conditions of ageing, the dry conditions impose carbonation that is three times more extensive than under wet conditions. This can be related to (i) the most important concentration of CO_2 in dry CO_2 experiments; (ii) the transport mechanisms of CO_2 and ions in the different media (supercritical CO_2, water, porous network of cement and clays, network of micro-cracks in the caprock, induced fracturing of the cement sheath); (iii) the different availability of CO_2 for the chemical reactions between dissolved species and supercritical phase; (iv) the local environment: under dry conditions, the water is interstitial or porous water with a weak mobility and thus implying local equilibria.

6. Summary and Conclusions

This study highlights the effect of CO_2 on the mechanical and mineralogical evolution of a Portland cement and clayey caprock/interfaces under geological conditions of storage. At least three steps of carbonation are observed, implying a chemical evolution of the solution which is assumed to be strongly dependent on the Mg/Ca ratio. The different episodes of alteration lead to two phases of cracking: the first affecting the caprock/cement interface, and the second inducing the impairment of the cement sheath. In both cases, the late precipitation of aragonite suggests a possible self-healing of cracks. The comparison between dry and wet experiments shows the main common mechanisms of alteration: carbonate precipitation, CSH leaching, and cracking, which is not observed from blank experiments performed with N_2. However, it demonstrates that dry CO_2 implies a stronger carbonation of the cement phase and limited transport of reacting species, in comparison with experiments in aqueous solution.

The interpolation of these results to the real case of storage has to be cautious because, in particular, the effect of the mechanical stress is not modelled here. However, this work gives new information on the chemical and mineralogical transformation of the caprock/cement interface and shows how cathodoluminecence is complementary to SEM or Raman mapping and can bring new insights to understanding the mineralogical evolution of rocks and cements.

Author Contributions: Emmanuel Jobard and Jérôme Sterpenich wrote the paper; Jérôme Sterpenich, Emmanuel Jobard, Jacques Pironon, Jérôme Corvisier and Aurélien Randi conceived and designed the experiments; Jérôme Sterpenich, Emmanuel Jobard and Jérôme Corvisier analyzed and interpreted the data.

Acknowledgments: This work was financially supported by the French Agency for Research through the projects ANR Injectivité (ANR-05-CO2-007) and ANR Interfaces (ANR-08-PCO2-006). The authors would like to acknowledge Ludovic Mouton and Sandrine Mathieu (SCMEM-GeoRessources laboratory, Université de Lorraine, France) for the technical assistance.

Conflicts of Interest: The authors declare no conflict of interest. The founding sponsors had no role in the design of the study; in the collection, analyses, or interpretation of data; in the writing of the manuscript, and in the decision to publish the results.

References

1. Loizzo, M.; Akemu, O.A.; Jammes, L.; Desroches, J.; Lombardi, S.; Annunziatellis, A. Quantifying the Risk of CO_2 Leakage Through Wellbores C1—SPE. *SPE Drill. Complet.* **2011**, *26*, 324–331. [CrossRef]
2. Carey, J.W.; Wigand, M.; Chipera, S.J.; WoldeGabriel, G.; Pawar, R.; Lichtner, P.C.; Wehner, S.C.; Raines, M.A.; Guthrie, G.D., Jr. Analysis and performance of oil well cement with 30 years of CO_2 exposure from the SACROC Unit, West Texas, USA. *Int. J. Greenh. Gas Control* **2007**, *1*, 75–85. [CrossRef]
3. Contraires, S.; Loizzo, M.; Lecampion, B.; Sharma, S. Long-term well bore integrity in Otway: Integrating ultrasonic logs, cement petrophysics, and mechanical analysis. *Energy Procedia* **2009**, *1*, 3545–3552. [CrossRef]
4. Xiao, T.; McPherson, B.; Bordelon, A.; Viswanathan, H.; Dai, Z.; Tian, H.; Esser, R.; Jia, W.; Carey, W. Quantification of CO_2-cement-rock interactions at the well-caprock-reservoir interface and implications for geological CO_2 storage. *Int. J. Greenh. Gas Control* **2017**, *63*, 126–140. [CrossRef]

5. Kutchko, B.G.; Strazisar, B.R.; Lowry, G.V.; Dzombak, D.A.; Thaulow, N. Rate of CO_2 Attack on Hydrated Class H Well Cement under Geologic Sequestration Conditions. *Environ. Sci. Technol.* **2008**, *42*, 6237–6242. [CrossRef] [PubMed]
6. Duguid, A.; Radonjic, M.; Scherer, W.G. Degradation of cement at the reservoir/cement interface from exposure to carbonated brine. *Int. J. Greenh. Gas Control* **2011**, *5*, 1413–1428. [CrossRef]
7. Sterpenich, J.; Jobard, E.; El Hajj, H.; Pironon, J.; Randi, A.; Caumon, M.-C. Experimental study of CO_2 injection in a simulated injection well: The MIRAGES experiment. *Greenh. Gases Sci. Technol.* **2014**, *4*, 210–224. [CrossRef]
8. Chavez Panduro, E.A.; Torsæter, M.; Gawel, K.; Bjørge, R.; Gibaud, A.; Yang, Y.; Bruns, S.; Zheng, Y.; Sørensen, H.O.; Breiby, D.W. In-Situ X-ray Tomography Study of Cement Exposed to CO_2 Saturated Brine. *Environ. Sci. Technol.* **2017**, *51*, 9344–9351. [CrossRef] [PubMed]
9. Cao, P.; Karpyn, Z.T.; Li, L. Dynamic alterations in wellbore cement integrity due to geochemical reactions in CO_2-rich environments. *Water Resour. Res.* **2013**, *49*, 4465–4475. [CrossRef]
10. Walsh, S.D.C.; Mason, H.E.; Du Frane, W.L.; Carroll, S.A. Mechanical and hydraulic coupling in cement-caprock interfaces exposed to carbonated brine. *Int. J. Greenh. Gas Control* **2014**, *25*, 109–120. [CrossRef]
11. Mito, S.; Xue, Z.; Satoh, H. Experimental assessment of well integrity for CO_2 geological storage: Batch experimental results on geochemical interactions between a CO_2-brine mixture and a sandstone-cement-steel sample. *Int. J. Greenh. Gas Control* **2015**, *39*, 420–431. [CrossRef]
12. Jung, H.B.; Kabilan, S.; Carson, J.P.; Kuprat, A.P.; Um, W.; Martin, P.; Dahl, M.; Kafentzis, T.; Varga, T.; Stephens, S.; et al. Wellbore cement fracture evolution at the cement-basalt caprock interface during geologic carbon sequestration. *Appl. Geochem.* **2014**, *47*, 1–16. [CrossRef]
13. Kjøller, C.; Torsæter, M.; Lavrov, A.; Frykman, P. Novel experimental/numerical approach to evaluate the permeability of cement-caprock systems. *Int. J. Greenh. Gas Control* **2016**, *45*, 86–93. [CrossRef]
14. Newell, D.L.; Carey, J.W. Experimental evaluation of wellbore integrity along the cement-rock boundary. *Environ. Sci. Technol.* **2012**, *47*, 276–282. [CrossRef] [PubMed]
15. Manceau, J.C.; Tremosa, J.; Audigane, P.; Lerouge, C.; Claret, F.; Lettry, Y.; Fierz, T.; Nussbaum, C. Well integrity assessment under temperature and pressure stresses by a 1:1 scale wellbore experiment. *Water Resour. Res.* **2015**, *51*, 6093–6109. [CrossRef]
16. Kutchko, B.G.; Strazisar, B.R.; Lowry, G.V.; Thaulow, N. Degradation of Well Cement by CO_2 under Geologic Sequestration Conditions. *Environ. Sci. Technol.* **2007**, *41*, 4787–4792. [CrossRef] [PubMed]
17. Brandvoll, Ø.; Regnault, O.; Munz, I.A.; Iden, I.K.; Johansen, H. Fluid-solid interactions related to subsurface storage of CO_2 Experimental tests of well cement. *Energy Procedia* **2009**, *1*, 3367–3374. [CrossRef]
18. Barlet-Gouédard, V.; Rimmelé, G.; Porcherie, O.; Quisel, N.; Desroches, J. A solution against well cement degradation under CO_2 geological storage environment. *Int. J. Greenh. Gas Control* **2009**, *3*, 206–216. [CrossRef]
19. Angeli, M.; Soldal, M.; Skurtveit, E.; Aker, E. Experimental percolation of supercritical CO_2 through a caprock. *Energy Procedia* **2009**, *1*, 3351–3358. [CrossRef]
20. Rutqvist, J.; Tsang, C.F. A study of caprock hydromechanical changes associated with CO_2-injection into a brine formation. *Environ. Geol.* **2002**, *42*, 296–305. [CrossRef]
21. Bildstein, O.; Jullien, M.; Crédoz, A.; Garnier, J. Integrated modeling and experimental approach for caprock integrity, risk analysis, and long term safety assessment. *Energy Procedia* **2009**, *1*, 3237–3244. [CrossRef]
22. Credoz, A.; Bildstein, O.; Jullien, M.; Raynal, J.; Pétronin, J.-C.; Lillo, M.; Pozo, C.; Geniaut, G. Experimental and modeling study of geochemical reactivity between clayey caprocks and CO_2 in geological storage conditions. *Energy Procedia* **2009**, *1*, 3445–3452. [CrossRef]
23. Wigand, M.; Kaszuba, J.P.; Carey, J.W.; Hollis, W.K. Geochemical effects of CO_2 sequestration on fractured wellbore cement at the cement/caprock interface. *Chem. Geol.* **2009**, *265*, 122–133. [CrossRef]
24. Duguid, A. An estimate of the time to degrade the cement sheath in a well exposed to carbonated brine. *Energy Procedia* **2009**, *1*, 3181–3188. [CrossRef]
25. Descostes, M.; Blin, V.; Bazer-Bachi, F.; Meier, P.; Grenut, B.; Radwan, J. Diffusion of anionic species in Callovo-Oxfordian argillites and Oxfordian limestones (Meuse/Haute–Marne, France). *Appl. Geochem.* **2007**, *23*, 655–677. [CrossRef]
26. Wileveau, Y.; Bernier, F. Similarities in the hydromechanical response of Callovo-Oxfordian clay and Boom Clay during gallery excavation. *Phys. Chem. Earth Parts A/B/C* **2008**, *33*, S343–S349. [CrossRef]

27. Tournassat, C.; Chainet, F.; Greneche, J.M.; Betelu, S.; Hadi, J.; Gaucher, E.; Charlet, L.; Ignatiadis, I. Probing Fe (III)/Fe(II) redox potential in a clayey material. In Proceedings of the 4th International Meeting Clays in Natural & Engineered Barriers for Radioactive Waste Confinement, Nantes, France, 29 March–1 April 2010.
28. El Hajj, H.; Abdelouas, A.; Grambow, B.; Martin, C.; Dion, M. Microbial corrosion of P235GH steel under geological conditions. *Phys. Chem. Earth* **2010**, *35*, 248–253. [CrossRef]
29. Jacquemet, N.; Pironon, J.; Caroli, E. A new experimental procedure for simulation of H_2S + CO_2 geological storage. Application to well cement aging. *Oil Gas Sci. Technol.* **2005**, *60*, 183–2006. [CrossRef]
30. Richter, D.K.; Götte, T.; Götze, J.; Neuser, R.D. Progress in application of cathodoluminescence (CL) in sedimentary petrology. *Mineral. Petrol.* **2003**, *79*, 127–166. [CrossRef]
31. Boggs, S.; Krinsley, D. *Application of Cathodoluminescence Imaging to the Study of the Sedimentary Rocks*; Cambridge University Press: Cambridge, UK, 2006.
32. De Choudens-Sanchez, V.; Gonzales, L. Calcite and aragonite precipitation under controlled instantaneous supersaturation: Elucidating the role of $CaCO_3$ saturation state and Mg/Ca ratio on calcium carbonate polymorphism. *J. Sediment. Res.* **2009**, *79*, 363–376. [CrossRef]
33. Jobard, E. Modélisation Expérimentale du Stockage Géologique du CO_2: Etude Particulière des Interfaces Entre Ciment du Puits, Roche Réservoir et Roche Couverture. Ph.D. Thesis, Université de Lorraine, Lorraine, France, 2013; p. 223. Available online: http://docnum.univ-lorraine.fr/public/DDOC_T_2013_0013_JOBARD.pdf (accessed on 15 May 2018).
34. Huet, B.; Tasoti, V.; Khalfallah, I. A review of Portland cement carbonation mechanisms in CO_2 rich environment. *Energy Procedia* **2011**, *4*, 5275–5282. [CrossRef]
35. Andac, M.; Glasser, F.P. Long-term leaching mechanisms of Portland cement-stabilized municipal waste fly ash in carbonated water. *Cem. Concr. Res.* **1999**, *29*, 179–186. [CrossRef]
36. Barlet-Gouédard, V.; Rimmelé, G.; Goffé, B.; Porcherie, O. Mitigation strategies for the risk of CO_2 migration through wellbores. In Proceedings of the IADC/SPE Drilling Conference, Miami, FL, USA, 21–23 February 2006.
37. Rimmelé, G.; Barlet-Gouédard, V.; Porcherie, O.; Goffé, B.; Brunet, F. Heterogeneous porosity distribution in Portland cement exposed to CO_2-rich fluids. *Cem. Concr. Res.* **2008**, *38*, 1038–1048. [CrossRef]